Research Article

Synthesis, Characterization, Fluorescence and Antimicrobial studies of Cu(II), Co(II), Ni(II), Zn(II) and Cd(II) complexes derived from Schiff's base (*E*)-2-(5-chloro-2-hydroxybenzylidene)-*N*-(4-phenylthiazol-2-yl)hydrazinecarboxamide

Fazlur Rahaman[ab*], Priti Gupta[ab*], Manjunatha M N[cb] , Prabhat Gautam[ab] and Subrata Monadal[ab]

[a]Department of Chemistry, CMR Institute of Technology, Bengaluru, Karnataka, India – 560 037
[b]VTU-RC affliated to Visweswaraya Technological University, Belgavi, Karnataka, India – 590 018
[c]Department of Chemistry, Ramaiah Institute of Technology, Bengaluru, Karnataka, India – 560 054
[ab]*fazlur.r@cmrit.ac.in & rahaman216@gmail.com*
[ab]*priti.g@cmrit.ac.in & pritigupta.ncl@gmail.com*
[cb]*mnmanjunathmsrit@gmail.com*
[ab]*prabhatgautam28@gmail.com*
[ab]*subratakatwa@gmail.com*

Abstract:

A series of Cu(II), Co(II), Ni(II), Zn(II) and Cd(II) complexes of (*E*)-2-(5-chloro-2-hydroxybenzylidene)-*N*-(4-phenylthiazol-2-yl)hydrazinecarboxamide **(HL)** with ONO donor ligand was synthesized. The ligand **(HL)** was prepared by the condensation of *N*-(4-phenylthiazol-2-yl)hydrazinecarboxamide with 5-chloro-2-hydroxybenzaldehyde. The **HL** and its metal complexes have been characterized using elemental analysis and various spectral techniques such as, FTIR, ^{1}H and ^{13}C NMR, Mass, UV–Visible, ESR, thermal analysis (TGA), magnetic moment, conductivity and powder-XRD. The Powder XRD pattern indicates hexagonal or tetragonal system for **HL** and its metal complexes. The fluorescence studies exhibits strong emission in the range of 400-500 nm for **HL**. Further in comparison the **HL**, Zn(II) and Cd(II) complexes showed enhanced emission whereas Cu(II), Co(II) and Ni(II) showed poor emission. The antimicrobial activities of the **HL** and its metal complexes were studied by minimum inhibitory concentration (MIC) method wherein the metal complexes showed better activity as compare to free ligand.

Key words: Schiff's base; Metal complexes; Antimicrobial; Fluorescence; Thiazole

1. Introduction

Transition metals are very reactive and exhibit excellent coordination properties due to which they can be utilized to form metal complexes with different organic ligands. The design and synthesis of such metal complexes has an important role in the development of coordination chemistry. Most of these compound show a broad spectrum of biological activities such as anti-inflammatory, anticonvulsant, antitubercular, antidepressant, antihistamine, cardiovascular, antidiabetic, anthelmintic, anti-allergic, antiviral, antifungal and antimicrobial activities [1]. Among the various building blocks, the thiazole moiety occupies key role in the development of organic ligands. The synthesis of thiazole derivatives is important due to their wide range of pharmaceutical and biological activities [2].

As a part of continuation of our research work in the field of coordination chemistry [3, 4] we became interested to synthesize the versatile Schiff base ligand having the thiazole moiety. Hydrazones are one of the member of azomethine class having >C=N-N< group with interlinked nitrogen atom. They are usually obtained by condensation of hydrazides with aldehydes or ketones. Since hyrazones have potential donor groups, capable of coordinating through its N and O atoms and have varied coordination abilities, thus they are of a special interest to coordination chemists [5-7]. These interesting properties of hydrazone and thiazole moiety has attracted our attention and aroused our interest in synthesizing the ligand containing thiazole moiety and elucidating the structure of its metal complexes. We hereby report a synthesis and structure elucidation of metal complexes of ligand (*E*)-2-(5-chloro-2-hydroxybenzylidene)-*N*-(4-phenylthiazol-2-yl)hydrazine carboxamide **(HL) (1)** [H refers to phenolate][8].

2. Experimental

2.1. Analysis and physical measurements

Elemental analyses were obtained using HERAEUS CHN-O rapid analyzer and metal analyses were carried out by following the standard methods. The IR spectra of the synthesized compounds were recorded as KBr pellets on PERKIN-ELMER Spectrum One FT-IR spectrometer, ^{1}H and ^{13}C NMR spectra were recorded on a BrukerAvance 400MHz spectrometer and are reported in parts per million (δ) downfield relative to DMSO-d_6 as internal standard. ESI mass spectra were recorded on mass spectrometer equipped with ESI source having mass range of 4000 amu in quadruple and 20,000 amu in Tof and Fast atom bombardment (FAB) mass spectrum of the ligand was obtained on JEOLSX102/DA6000 mass spectrometer using Argon/Xenon as the gas. The accelerating voltage was 10kV and the spectrum was recorded at room temperature using meta-dinitrobenzyl alcohol as a matrix. UV-Visible spectra of the complexes were recorded on Elico-SL 164 double beam UV-Visible spectrophotometer in the range 200–1200 nm in dimethylformamide (DMF) solution (1×10^{-3}M). TGA studies were carried out by using Perkin Elmer TGA 7 with 20 ºC per minutes of N_2, controller from 28 ºC to 1200 ºC. Electron paramagnetic resonance (EPR) measurements were carried out on a Bruker Biospin Gmbh spectrometer working at a microwave frequency of 9.4GHz using diphenylpicrylhydrazide (DPPH) as a reference with the field set at 3200 Gauss.

2.2. Materials and methods

All the chemicals are of analytical reagent grade and the solvents were purified according to standard methods [9]. The precursor 4-phenylthiazole-2-semicarbazide is synthesized by reported method [10, 11]. The metal (II) hydrates are used as such procured. The metal and chloride content were determined as per the standard methods [9].

2.3. Synthesis of ligand (HL)

The mixture of *N*-(4-phenylthiazol-2-yl)hydrazinecarboxamide **(2)** (1 mmol) and 5-chloro-2-hydroxybenzaldehyde **(3)** (1 mmol) was dissolved in 30 mL of absolute ethanol followed by addition of sodium polyacrylate (SPA) and 2 drops of H_2SO_4 . The solution was refluxed for 4 h. The reaction mixture was cooled to room temperature, filtered, dried and recrystallized from THF to obtain **HL (Scheme 1).**

[$C_{17}H_{13}N_4O_2SCl$]: Colourless Solid. Yield 80% m.p. 225 °C. Anal. Calc for $C_{17}H_{13}N_4O_2SCl$ (MW: 372.83): C-54.77; H-3.51; N-15.03; Cl; 9.51% Found: C-54.73; H-3.47; N-14.99; 9.35%, IR data (ν cm^{-1}, KBr): ν(NH amide) 3201; ν(NH thiazole) 3102; ν(O-H) 2895, ν(C=O) 1674; ν(C=N) 1600; ν(C-O

phenolic) 1257; ν(C-S-C) 691; ^{1}H NMR (DMSO-d_6, 400 MHz) δ 6.90 (d, 1H, *J* = 8.8 Hz), δ 7.23-7.26 (m, 1H), δ7.30-7.33 (m, 1H), δ 7.39-7.46 (m, 2H), δ7.56 (s, 1H), δ 7.94-7.96 (m, 2H), δ 8.27 (s, 2H), δ 10.29 (s, 1H), δ 11.15 (s, 1H), δ 11.22 (s, 1H); ^{13}C NMR (DMSO-d_6, 400 MHz): δ 107.7, 117.6, 122.1, 123.3, 125.5, 125.7, 126.1, 127.6, 128.6, 130.3, 134.5, 148.9, 154.9, 159.2; HRMS(ESI) m/z for $C_{17}H_{13}N_4O_2SCl$ calcd $(M+Na)^+$ 395.0345, found $(M+Na)^+$ 395.0348.

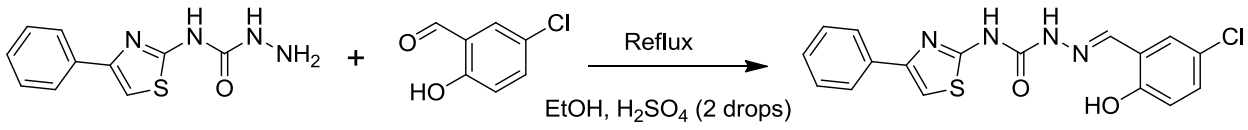

2 **3** **1**

Scheme-1

2.4. Preparation of Cu(II), Co(II), Ni(II), Zn(II) and Cd(II) complexes (1a-e)

The corresponding metal chlorides (1 mmol) was dissolved in ethanol (10 mL) and added drop wise to the hot ethanolic solution (30mL) of the **HL (1)** (1 mmol) with constant stirring. The resulting solution was refluxed for 4 h followed by the addition of sodium acetate (0.5 g) to adjust the pH of the solution (calc. pH 7.0-7.5) and further refluxed for 2 h. The mixture was quenched by pouring into distilled water (80-100 ml) with constant stirring. Suspended solid complexes are allowed to settle, filtered, washed with sufficient quantity of distilled water and with hot ethanol and dried in a vacuum over anhydrous calcium chloride in a desiccator at room temperature.

[$Cu(C_{34}H_{24}Cl_2N_8O_4S_2)$]: Green Solid. Yield: 72%; mp. >300 °C. Anal. Calc for [$Cu(C_{34}H_{24}Cl_2N_8O_4S_2)$]: (MW: 807.19): C-50.59; H -3.00; N-13.88; Cl;8.78; Cu-7.87 %; Found: C-50.55; H-2.95; N-13.84; Cl; 8.62; Cu-7.83%, IR data (ν cm^{-1}, KBr): ν(NH amide) 3165; ν(NH thiazole) 3065; ν(C=O) 1642; ν(C=N) 1532; ν(C-O phenolic) 1280; ν(C-S-C)686 ; ν(M-O) 432; ν(M-N) 463; *m/z*;806.

[$Co(C_{34}H_{24}Cl_2N_8O_4S_2)$]: Brown Solid. Yield: 71%; m.p. >300°C. Anal. Calc for [$Co(C_{34}H_{24}Cl_2N_8O_4S_2)$]: (MW: 802.57): C-50.88; H -3.01; N-13.96; Cl;8.83; Co-7.34%; Found: C-50.83; H-2.97; N-13.92; Cl;8.71; Co-7.31%, IR data (ν cm^{-1}, KBr): ν(NH amide) 3238; ν(NH thiazole) 3069; ν(C=O) 1601; ν(C=N) 1535; ν(C-O phenolic) 1272; ν(C-S-C)698 ; ν(M-O) 420; ν(M-N) 457: *m/z*;802.

[$Ni(C_{34}H_{24}Cl_2N_8O_4S_2)$]: Brown Solid. Yield: 74%; m.p. 282 °C. Anal. Calc for [$Ni(C_{34}H_{24}Cl_2N_8O_4S_2)$]: (MW: 802.33): C-50.90; H -3.02; N-13.97; Cl; 8.84; Ni-7.32%; Found: C-50.90; H-2.96; N-13.92; Cl; 8.72; Ni-7.27%, IR data (ν cm^{-1}, KBr): ν(NH amide) 3224; ν(NH thiazole) 3070; ν(C=O) 1645; ν(C=N) 1536; ν(C-O phenolic) 1275; ν(C-S-C)698 ; ν(M-O) 423; ν(M-N) 461:

[$Zn(C_{17}H_{12}Cl_2N_4O_2S)$]: Yellow Solid. Yield: 71%; m.p. 278 °C. Anal. Calc for [$Zn(C_{17}H_{12}Cl_2N_4O_2S)$]: (MW: 469.93): C-43.20; H – 2.56; N-11.85; Cl; 15.00; Zn-13.83%; Found: C-40.10; H-3.14; N-11.94 ;Cl-14.81; Zn-12.82%, IR data (ν cm^{-1}, KBr): ν(NH amide) 3115; ν(NH thiazole) 3055; ν(C=O) 1618; ν(C=N) 1532; ν(C-O phenolic) 1280; ν(C-S-C)695 ;ν(M-O) 409; ν(M-N) 462; ν(M-Cl) 314: *m/z*;472.

[$Cd(C_{17}H_{12}Cl_2N_4O_2S)$]: Yellow Solid. Yield: 70%; m.p. >300°C. Anal. Calc for [$Cd(C_{17}H_{12}Cl_2N_4O_2S)$]: (MW: 519.68): C-39.29; H -2.33; N-10.78; Cl-13.64; Cd-21.63 %; Found: C-36.69; H-2.86; N-10.00; Cl-13.57; Cd-20.18%, IR data (ν cm^{-1}, KBr): ν(NH amide) 3273; ν(NH thiazole) 3045; ν(C=O) 1662; ν(C=N) 1577; ν(C-O phenolic) 1268; ν(C-S-C)703 ;ν(M-O) 410; ν(M-N) 505; ν(M-Cl) 312: ^{1}H NMR (d_6-DMSO; δ ppm); δ 6.90 (d, 1H, *J* = 8.8 Hz), 8.95 (s, 1H, azomethine C=NH); 6.92-8.27 (m, 9H, ArH); 11.10 (s, 1H CONH); 10.25 (s, 1H CONH); *m/z*;520.

2.5. Biological Evaluation

The antimicrobial activity of **HL (1)** and its metal complexes **(1a-e)** was performed by the MIC [12]. The antibacterial activity were done by using gram positive organism *Staphylococcus aureus* and gram negative organism *Escherichia coli* while *Aspergillus niger* & *Candida albicans* were used for antifungal activity at 1mg/mol concentrations in solvent DMF used as control. The bacteria are sub-cultured in agar medium. The Petri plates were incubated for 24 h at 37 ˚C, for comparison screening of standard antibacterial drug streptomycin was also carried out under similar conditions. The fungi were sub-cultured in potato dextrose agar (PDA) and standard antifungal drug grisofluvin used for comparison.

3. Result and Discussion

The general composition for the metal complexes was found to be [M(L)] where M= Zn(II) and Cd(II) and $[M(L)_2]$ where M=Cu(II), Ni(II) and Co(II). The C, H and N analysis data of all the metal complexes are in good agreement with the calculated values. The elemental analysis data and melting points are listed in **(Table 1).** The complexes obtained were coloured, polycrystalline, air stable and insoluble in common organic solvents but readily soluble in DMF and DMSO.

3.1. FT-IR Spectral studies

The IR spectra of ligand **HL** exhibited characteristic medium to strong intensity bands in the region 3201 cm^{-1} and 3102 cm^{-1} due to the amide $\nu_{NH/NH}$ vibrations. In the present investigation the band due to hydrogen bonded –OH group was observed at 2895 cm^{-1}. A strong band observed at 1674 cm^{-1} is attributed to $\nu_{C=O}$ of the carbonyl function. The medium intensity sharp band observed at 1600 cm^{-1} is assigned to $\nu_{C=N}$ group. An intense band at 691cm^{-1} is due to the characteristic vibrations of the ν_{C-S-C} thiazole ring while the high intensity band observed at 1257 cm^{-1} is assigned to the phenolic ν_{C-O} vibration [11, 13].

The disappearance of weak band in the ligand (**HL),** which was appeared at 2895 cm^{-1} indicated the deprotonation of intramolecular hydrogen bonded phenolic –OH group upon complexation with metal ions. The band due to $\nu_{C=N}$ is observed in the ligand (**HL)** at 1600 cm^{-1} shows a negative shift of 23-68 cm^{-1} and appeared in the region 1577-1532 cm^{-1} in all the metal complexes, confirms the coordination through the azomethine nitrogen atom. However, the C-S-C characteristic vibration band due to thiazole ring observed in all the complexes in the range 703-686 cm^{-1} showed no considerable shift in its position as compared to ligand thus ruling out the possibility of coordination of ring sulfur to the metal ions in these complexes. The band due to $\nu_{C=O}$ is observed in the ligand at 1674 cm^{-1}, showed a negative shift of 9-73 cm^{-1} and appeared in the region 1665-1601 cm^{-1} in all the metal complexes, which indicate the involvement of carbonyl oxygen in the complexation with metal ion. The bands due to NH/NH observed at 3201/3102 cm^{-1} in case of ligand **(HL)** were found to be in the range 3238-3115 cm^{-1} and 3084-3045 cm^{-1} in all the complexes, confirms that during complexation enolisation of carbonyl group has not taken place and thereby NH/NH remain intact in all the complexes[13].

Due to interference of the ligand vibrations, assignment of the band to various ν_{M-O} and ν_{M-N} vibrations in the lower frequency region appears to be complicated. The low frequency skeletal vibrations due to M-O and M-N stretching provide direct evidence for the complexation. In the present complexes the bands in the region 406-432 cm^{-1} and 525-457 cm^{-1} have been assigned for ν_{M-O} and ν_{M-N} vibrations respectively[14, 15]. The bands in the region 305-315 cm^{-1} have been assigned to M-Cl bands in the case of Zn(II) and Cd(II) complexes[16].

3.2. ^{1}HNMR spectral studies

The ^{1}HNMR spectra of the ligand **(HL)** and its Cd (II) **(1e)** complex were recorded in DMSO-*d6* as solvent. The ^{1}HNMR spectra of the ligand **(HL)** showed a doublet at δ 6.90 (d, 1H, *J* = 8.8 Hz) due to aromatic proton of phenyl ring adjacent to C-OH group. The four aromatic protons of 4-phenylthiazole and phenyl ring have appeared in the region δ 7.23-7.46 as multiplets. The singlet at δ 7.56 (s, 1H), is due to proton of thiazole ring. A multiplet at δ 7.94-7.96 (m, 2H) is attributed to the two aromatic proton of phenylthiazole ring. A singlet of two proton at δ 8.27 (s, 2H) is attributed to the azomethine and proton adjacent to C-Cl group. A proton due to –OH group at 2-positon of the salicylaldehyde ring has resonated as a singlet at δ 11.22 (s, 1H). The two-amide protons of –NHCONH have appeared as distinct singlets at δ 11.15 (s, 1H) and δ 10.29 (s, 1H) respectively.

In the ^{1}HNMR spectrum of the Cd (II) **(1e)** complex **(Figure S2)** showed a doublet at δ 6.90 (d, 1H, *J* = 8.8 Hz) is due to aromatic proton of phenyl ring adjacent to C-OH group. In case of ligand **(HL)** proton due to –OH group at 2-positon of the salicylaldehyde ring has resonated as a singlet at δ 11.22 (s, 1H) has been disappeared in Cd (II) complex indicating the complexation via deprotonation. The singlet due to azomethine proton shifted to down field and appeared at 8.95 in the case of complex. Remaining eight aromatic protons appeared in the region 6.92 -8.27.

3.3. Mass Spectral Studies

The ligand **(HL)** and its Cu(II), Co(II), Zn(II) and Cd(II) complexes have been studied for their mass spectral studies **(Table-2).** The high resonance mass spectrum of ligand **(HL)** showed a molecular ion peak recorded at m/z 395.0348 (M+Na), which is equivalent to its molecular weight (M.W. = 372) **(Figure S1)**. The FAB mass spectra of Cu(II) **(1a)**, Co(II) **(1b)**, Zn(II) **(1d)** and Cd(II) **(1e)** complexes are depicted in supplementary data (Figure S2, S3, S4 & S5). The molecular ion (M-1) peak for Cu (II) and Co(II) complexes **(1a & b)** was observed at (m/z) 806 & 802, which are equivalent to their molecular mass and confirms the 1:2 (M:L) stoichiometry. Whereas the spectra of Zn(II) and Cd(II) complexes **(1d & e)** shows the molecular ion peaks (M-1) (m/z) at 472 & 520 which gives the confirmation of 1:1 (M:L) stoichiometry.

3.4. Nature and Stoichiometry of the complexes

The elemental analysis and physico-chemical techniques, shows that the complexes Zn(II) and Cd(II) form 1:1 (M:L) stoichiometry with the empirical formula $[M(L)Cl_2]$ whereas Cu(II), Ni(II) and Co(II) complexes exhibited 1:2 stoichiometry with the empirical formula $[M(L)_2]$. Based on analytical data and spectral studies, proposed structures for all the metal complexes are shown in **Figure 1.**

The conductivity measurements in DMF solution at a concentration of $1x10^{-3}$ M **(Table 1)** shows low molar conductance value for the synthesized metal complexes, which accounts for the non-dissociative and non-electrolytic nature of these complexes in DMF.

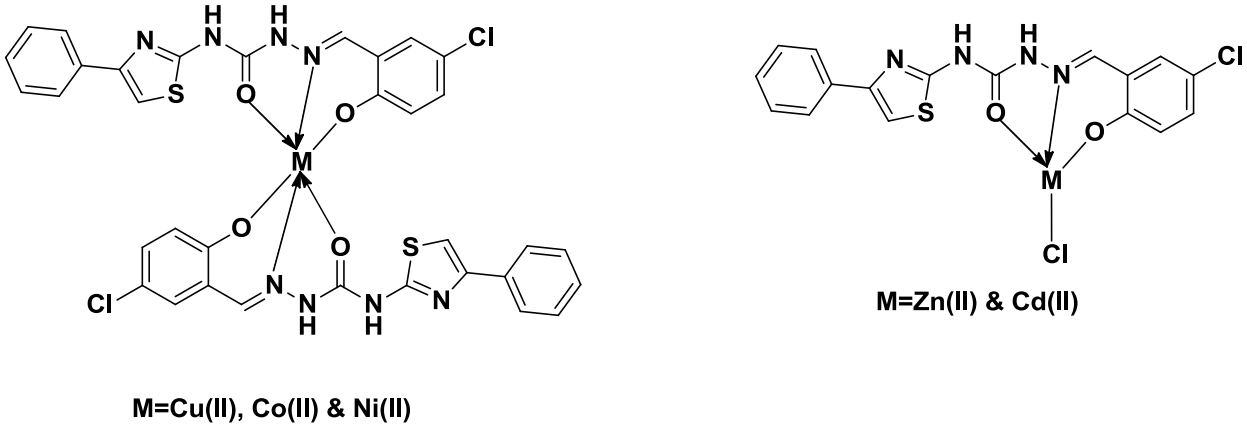

Figure 1: Proposed structures for the metal complexes

3.5. Electronic and magnetic susceptibility data

The UV-visible spectra for **HL** and its various complexes were recorded in DMF solution keeping a fixed concentration of 10^{-3} M. The ligand **(HL)** shows three bands at 35714 cm^{-1}, 30120 cm^{-1}, & 29154 cm^{-1} due to $\pi\rightarrow\pi^*$ and $n\rightarrow\pi^*$ transitions. The electronic absorption spectrum of the Cu(II) **(1a)** complex shows three bands at 13397-187689 cm^{-1} assigned to the $^2B_{1g} \rightarrow {}^2E_g$, $^2B_{2g}$ and $^2A_{1g}$ transitions in distorted octahedral geometry of **1a** [17]. The observed magnetic moment value for the **1a** is 1.83 B.M. In view of the above observations the present **1a** complex is expected to have distorted octahedral geometry. The electronic spectrum of Ni (II) **(1c)** complex exhibited three bands in the region 10631, 17145 and 24254 cm^{-1} are attributed to $^3A_{2g}(F) \rightarrow {}^3T_{2g}(F)(\nu_1)$, $^3A_{2g}(F) \rightarrow {}^3T_{1g}(F)\ (\nu_2)$ and $^3A_{2g}(F) \rightarrow {}^3T_{1g}(P)\ (\nu_3)$ transitions respectively. Moreover, the ν_2/ν_1 ratio in the range of 1.56-1.61 is indicative of octahedral stoichiometry for the Ni(II) **(1c)** complex[18, 19]. The magnetic moment value for **1c** complex is 2.98 B.M, which is in well agreement with the expected value for octahedral geometry around the central metal ion[20]. The electronic spectrum of Co (II) **(1b)** complex displayed three well defined bands in the region 8646 cm^{-1}, 17144 cm^{-1} & 20612 cm^{-1} due to the $^4T_{1g}(F) \rightarrow {}^4T_{2g}(F)\ (\nu_1)$, $^4T_{1g}(F) \rightarrow {}^4A_{2g}(F)\ (\nu_2)$ and $^4T_{1g}(F) \rightarrow {}^4T_{1g}(P)\ (\nu_3)$ transitions respectively. These transitions also suggest the octahedral geometry for **1b** complex [18]. The measured magnetic moment value for **1b** is 4.77 B.M, which suggests octahedral geometry. The measured

value is observed in the expected range for μ_s and μ_{s+1} due to the partial quenching of orbital contribution to the magnetic movement [21].

3.6. ESR Studies

The solid state X band ESR spectrum of C(II) **1a** complex (Figure S8) was recorded in polycrystalline sample in acetonitrile solution at the frequency of 9.4 GHz under a magnetic field strength 3200G. The calculated spin Hamiltonian parameters of **1a** gives $g_{\parallel}$ (2.22) > $g_{\perp}$ (2.01) > 2.0023 which shows that the complex is axially symmetric and copper site has a $dx^2–y^2$ ground state characteristic of octahedral geometry[22]. According to Hathaway and Billing[23], if the G value is found to be greater than 4, which suggest that the exchange interaction between the copper ions is negligible in solid state, whereas when it is less than 4 a considerable exchange interaction is indicated in the solid complex. In this case the calculated G value is found to be 4.682 for 1a complex, suggesting that there is no copper-copper exchange interactions[22, 24]. According to Hathaway and Billing[23], the G value is found to be 4.682 for 1a complex, suggesting that there is no copper-copper exchange interactions[22, 24].

3.7. TGA Studies

The thermogram of Ni(II) **(1b)** complex, shows the first stage decomposition corresponding to the weight loss of NH_3 molecule at 140 ºC. The theoretical weight loss for the decomposition was 2.12%, which is in agreement with the observed value 2%. Further complex underwent degradation at 336°C with a weight loss of 11.81%, which is attributed to the decomposition of HCN and HCl species. This practical weight loss of 11.81% is in good agreement with theoretical weight loss of 11.73%. The third stage decomposition at 440°C, with weight loss of 58.66%, resembles to the decomposition of $C_{22}H_{14}N_5OS$ species. This practical weight loss 58.66% is in accordance with theoretical weight loss of 59.39%. Thereafter the compound showed a gradual decomposition up to 1100°C and onwards. The probable assignments are given in the **Table 3.**

3.8. X-ray powder diffraction studies

We have carried out powder X-ray diffraction studies for ligand **HL** and its all the metal complexes in the range of 5- 90º (2θ). All the compounds were found to be amorphous. The interplanar spacing (d) has been calculated from the powder-XRD pattern using Bragg's equation from the position of intense peaks and has been provided in Table **4-8** and the powder XRD pattern shown in Figure-2.

The ligand (**HL)** shows various reflections ranging from 5-90º (2θ) and the interplanar spacing (d) has been calculated from the position of intense peaks using Bragg's relation. The calculated d-spacing and relative intensities with respect to most intense peaks have been recorded in Table-**S1**. The maximum intensity of the peak for the compound was found to be at 2θ =21.82º which corresponds to d-spacing value 21.15026 Å. The $(h^2+k^2+l^2)$ values are 3, 9, 12, 14, 16, 20, 23, 25, 27, 28, 30, 33, 37, 42, 48, 49, 58, 60, 64 and 91. The occurrence of forbidden numbers 23, 28 and 60 indicates the ligand **HL** may belong to hexagonal or tetragonal system[25, 26].

Similarly for Cu(II) (1a), Co(II) (1b), Ni(II) (1c), Zn(II) (1d) and Cd(II) (1e) complexes, the d-spacing and other lattice parameters have calculated with respect to most intense peaks as shown in Table **S2-S6**. The presence of forbidden number 28, 31, 39 in both Co(II) and Zn(II) complexes while 7 for Cu(II) and Ni(II) complexes indicates the complexes may belong to hexagonal or tetragonal system. However in case of Cd (II) complex, the absence of such forbidden number indicate the cubic system for the complex[25–27]. The particle size of all the compounds were calculated using Debye Sherrer's equation and has been found that ligand HL and its complexes are in nanometer dimension [Table-1].

3.9. Fluorescence Study

The fluorescence study of ligand **(HL)** and its various transition metal complexes was carried out in DMF at room temperature (Figure-3). HL exhibits a strong blue emission at 440 nm upon excitation at 374 nm. The fluorescence spectra of metal complexes shows significant change in emission behavior in contrast to fluorescence spectra of HL. The emission spectra show a dramatic fluorescence quenching for Cu(II) (1a), Co(II) (1b) and Ni(II) (1c) complexes with minute change in emission band position upon excitation in the range of 370-390 nm. The remarkable fluorescence quenching of HL upon complexation with the aforementioned metal ions (M:L = 1:2) may be attributed to decrease in electron density on Schiff base

[32, 33]. On the other hand, the fluorescence spectra of Zn(II) (1d) and Cd(II) (1e) complexes show enhanced emission compared to HL upon excitation at 378 nm and 371 nm respectively[28, 29]. In this case the complexation occurs via 1:1 ratio of Metal to ligand. The enhancement in the emission maxima follow the order as HL < Cd(II) < Zn(II).

3.10. Anti-microbial activity study

The antimicrobial activity data shows that the compounds exhibit antimicrobial properties and it is also important to note that some of the metal complexes showed more activity than parent ligand. The increase in activity of metals can be explained based on chelation theory[12].

The antibacterial data given in figure-4 indicates that, the free ligand molecule has shown less activity against both pathogens. The antibacterial activity of metal complexes against pathogens *S. aurus* and *E. coli in vitro* tests at MIC 1mg/mL as follows Co(II)>Ni(II)>Zn(II),Cd(II),>Cu(II)> HL. The antifungal activity results of ligand and its metal complexes against pathogens is evidence that complexes showed better activity than the parent ligand molecule. Based on their zone of inhibition against *A. niger* and *C. albicansin in vitro* tests at MIC of 1mg/mL as follows Zn(II)>Co(II)>Ni(II)>Cu(II)>Cd(II)>HL and Zn(II)>Co(II)>Ni(II),Cu(II)>Cd(II)>HL respectively[12, 30].

Conclusions

In the present study, the Schiff base, ligand (HL) and its Cu(II), Co(II), Ni(II), Zn(II) and Cd(II) complexes have been synthesized and explored. The bonding sites for the metal ions are the azomethine nitrogen, carbonyl and phenolic oxygen atoms. The ligand and its metal complexes showed enhanced antimicrobial activity compared with standard antifungal and antibacterial agents. All the synthesized compounds were characterized by various physico-chemical techniques such as IR, NMR, UV-Vis, ESR, TGA, Mass, powder XRD, elemental analysis and magnetic susceptibility data. All these data have justified the 1:1 type of stoichiometry with the empirical formula [M(L)Cl] for Zn(II), and Cd(II) complexes. The Cu(II), Co(II) and Ni(II) complexes exhibited 1:2 type of stoichiometry with the empirical formula $[M(L)_2]$.

Acknowledgement:

We are grateful to NMR Research Centre, IISc, Bengaluru, SAIF, Sophisticated Test and Instrumentation Centre, Kochi and SAIF, Central Drug Research Institute, Lucknow, for providing spectral analysis data. We are also thankful to Department of Microbiology, Gulbarga University for antimicrobial studies.

SUPPORTING INFORMATION:

^{1}HNMR, Mass, ESR, TGA and XRD spectra are provided in supporting information.

Reference

1. Abu-Dief AM, Mohamed IMA (2015) A review on versatile applications of transition metal complexes incorporating Schiff bases. Beni-Suef Univ J Basic Appl Sci 4:119–133. https://doi.org/10.1016/j.bjbas.2015.05.004
2. Neelakantan MA, Marriappan SS, Dharmaraja J, et al (2008) Spectral, XRD, SEM and biological activities of transition metal complexes of polydentate ligands containing thiazole moiety. Spectrochim Acta - Part A Mol Biomol Spectrosc 71:628–635. https://doi.org/10.1016/j.saa.2008.01.023
3. Rahaman F, Ijare OB, Jadegoud Y, Mruthyunjayaswamy BHM (2009) Phenoxo-bridged symmetrical homobinuclear complexes derived from an "end-off" compartmental ligand, 2,6-bis[5′-chloro-3′-phenyl-1H-indole-2′-carboxamidyliminomethyl]-4-methylphenol. J Coord Chem 62:1457–1467. https://doi.org/10.1080/00958970802600888
4. Rahaman F, Mruthyunjayaswamy BHM (2014) Synthesis, spectral characterization and biological activity studies of transition metal complexes of Schiff base ligand containing indole moiety. Complex Met 1:88–95. https://doi.org/10.1080/2164232x.2014.889580
5. Sharma VK, Srivastava S, Srivastava A (2006) Synthesis and spectroscopic studies of novel mononuclear and binuclear ruthenium(III) complexes with bidentate and tridentate acyclic hydrazones. J Coord Chem 59:1321–1334. https://doi.org/10.1080/00958970500473083
6. Mohanraj M, Ayyannan G, Raja G, Jayabalakrishnan C (2016) Synthesis, characterization, DNA binding, DNA cleavage, antioxidant and in vitro cytotoxicity studies of ruthenium(II) complexes containing hydrazone ligands. J Coord Chem 69:3545–3559. https://doi.org/10.1080/00958972.2016.1235700
7. Babahan I, Emirdaı-Öztürk S, Poyrazoılu-Çoban E (2015) Spectroscopic and biological studies of new mononuclear metal complexes of a bidentate NN and NO hydrazone-oxime ligand derived from egonol. Spectrochim Acta - Part A Mol Biomol Spectrosc 141:300–306. https://doi.org/10.1016/j.saa.2014.12.074
8. Mondal S, Gupta P, Rahaman F, et al (2021) Colorimetric and Fluorimetric Detection of Fluoride Ion Using Thiazole Derived Receptor. Spectrochim Acta Part A Mol Biomol Spectrosc 264:120301. https://doi.org/10.1016/j.saa.2021.120301
9. I VA (1968) Text Book of Quantitative Inorganic Analysis, 3rd ed. Longman ELBS, London, UK
10. Dodson RM, King LC (1945) The Reaction of Ketones with Halogens and Thiourea. J Am Chem Soc 67:2242–2243. https://doi.org/10.1021/ja01228a059
11. Basavarajaiah SM, Mruthyunjayaswamy BHM (2010) Synthesis and anti-microbial activity of (Z)-4-(4-substituted-thiazol-2-yl) -l-(2- oxoindolin-3-ylidene) semicarbazide and its derivatives. Indian J Chem - Sect B Org Med Chem 49:1117–1126. https://doi.org/10.1002/chin.201051125
12. Karekal MR, Biradar V, Bennikallu Hire Mathada M (2013) Synthesis, characterization, antimicrobial, DNA cleavage, and antioxidant studies of some metal complexes derived from Schiff base containing indole and quinoline moieties. Bioinorg Chem Appl 2013:. https://doi.org/10.1155/2013/315972
13. Yernale NG, Bennikallu Hire Mathada M (2020) Preparation of octahedral Cu(II), Co(II), Ni(II) and Zn(II) complexes derived from 8-formyl-7-hydroxy-4-methylcoumarin: Synthesis, characterization and biological study. J Mol Struct 1220:. https://doi.org/10.1016/j.molstruc.2020.128659
14. Nakamoto K (1978) Infrared and Raman Spectra of Inorganic and Coordination Compounds. Wiley and Sons, New York
15. Al-Saif FA, Refat MS (2012) Ten metal complexes of vitamin B3/niacin: Spectroscopic, thermal, antibacterial, antifungal, cytotoxicity and antitumor studies of Mn(II), Fe(III), Co(II), Ni(II), Cu(II), Zn(II), Pd(II), Cd(II), Pt(IV) and Au(III) complexes. J Mol Struct 1021:40–52. https://doi.org/10.1016/j.molstruc.2012.04.057
16. Rojo T, Arriortua MI, Ruiz J, et al (1987) Magnetostructural correlations in parallel square-planar chloride bridged copper(II) dimers: Structure, dynamic nuclear magnetic resonance study, and

magnetic properties of [Cu2(terpy)2Cl2][PF6]2. J Chem Soc Dalt Trans 285–291. https://doi.org/10.1039/DT9870000285
17. Mahendra Raj K, Vivekanand B, Nagesh GY, Mruthyunjayaswamy BHM (2014) Synthesis, spectroscopic characterization, electrochemistry and biological evaluation of some binuclear transition metal complexes of bicompartmental ONO donor ligands containing benzo[b]thiophene moiety. J Mol Struct 1059:280–293. https://doi.org/10.1016/j.molstruc.2013.12.010
18. Bhaskar RS, Ladole CA, Salunkhe NG, et al (2020) Synthesis, characterization and antimicrobial studies of novel ONO donor hydrazone Schiff base complexes with some divalent metal (II) ions. Arab J Chem 13:6559–6567. https://doi.org/10.1016/j.arabjc.2020.06.012
19. Singh K, Kumar Y, Puri P, et al (2012) Cobalt, nickel, copper and zinc complexes with 1,3-diphenyl-1H-pyrazole-4- carboxaldehyde Schiff bases: Antimicrobial, spectroscopic, thermal and fluorescence studies. Eur J Med Chem 52:313–321. https://doi.org/10.1016/j.ejmech.2012.02.053
20. Abd-Elzaher MM, Labib AA, Mousa HA, et al (2016) Synthesis, anticancer activity and molecular docking study of Schiff base complexes containing thiazole moiety. Beni-Suef Univ J Basic Appl Sci 5:85–96. https://doi.org/10.1016/j.bjbas.2016.01.001
21. Abd-Elzaher MM, Labib AA, Mousa HA, et al (2016) Synthesis, anticancer activity and molecular docking study of Schiff base complexes containing thiazole moiety. Beni-Suef Univ J Basic Appl Sci 5:85–96. https://doi.org/10.1016/j.bjbas.2016.01.001
22. Fouda MFR, Abd-Elzaher MM, Shakdofa MME, et al (2008) Synthesis and characterization of transition metal complexes of N′-[(1,5-dimethyl-3-oxo-2-phenyl-2,3-dihydro-1H-pyrazol-4-yl)methylene] thiophene-2-carbohydrazide. Transit Met Chem 33:219–228. https://doi.org/10.1007/s11243-007-9024-0
23. Hathaway BJ, Billing DE (1970) The electronic properties and stereochemistry of mono-nuclear complexes of the copper(II) ion. Coord Chem Rev 5:143–207. https://doi.org/10.1016/S0010-8545(00)80135-6
24. Emam SM, El Sayed IET, Nassar N (2015) Transition metal complexes of neocryptolepine analogues. Part I: Synthesis, spectroscopic characterization, and in vitro anticancer activity of copper(II) complexes. Spectrochim Acta - Part A Mol Biomol Spectrosc 138:942–953. https://doi.org/10.1016/j.saa.2014.03.114
25. Cullity B. D (1978) Elements of X-ray Difraction. Addison-Wesley Pub. Co
26. Eye, R.W.M.D., Wait E (1960) X-ray Powder Photography in Inorganic Chemistry. Butterworths, London
27. Swathy SS, Selwin Joseyphus R, Nisha VP, et al (2016) Synthesis, spectroscopic investigation and antimicrobial activities of some transition metal complexes of a [(2-hydroxyacetophenone)-3-isatin]-bishydrazone. Arab J Chem 9:S1847–S1857. https://doi.org/10.1016/j.arabjc.2012.05.004
28. Yamgar BA, Sawant VA, Sawant SK, Chavan SS (2009) Copper(II) complexes of thiazolylazo dye with triphenylphosphine and N3- or NCS- as coligands: Synthesis, spectral characterization, electrochemistry and luminescence properties. J Coord Chem 62:2367–2374. https://doi.org/10.1080/00958970902838339
29. Singh K, Kumar Y, Puri P, et al (2012) Thermal, Spectral, Fluorescence, and Antimicrobial Studies of Cobalt, Nickel, Copper, and Zinc Complexes Derived from 4-[(5-Bromo-thiophen-2-ylmethylene)-amino]-3-mercapto-6-methyl-5-oxo-[1,2,4]triazine. Int J Inorg Chem 2012:1–9. https://doi.org/10.1155/2012/873232
30. Raman N, Dhaveethu Raja J, Sakthivel A (2007) Synthesis, spectral characterization of Schiff base transition metal complexes: DNA cleavage and antimicrobial activity studies. J Chem Sci 119:303–310. https://doi.org/10.1007/s12039-007-0041-5

Table-1: Physical, Analytical, Magnetic susceptibility and Molar conductance data of Ligand (HL) and its Complexes.

Comp. No.	Empirical Formula/ Molecular formula	Mol. Wt.	M.P. Yield (^{0}C), (%)	Elemental Analysis (%) Calcd/(Found)					Mag. Moment μ_{eff}.(B.M.)	Molar Conductance (λ_M) ohm^{-1}cm^{2}mol^{-1}	Size in nm (using Debye Sherrer eqn)
				M	C	H	N	Cl			
HL(1)	$C_{17}H_{13}N_4O_2SCl$	372.83	232 (70)	--	54.77 (52.53)	3.51 (3.48)	15.03 (14.85)	9.51 (9.35)	--	--	32.54-34.22
1a	$[Cu(L)_2]$	807.19	>300 (62)	7.87 (7.75)	50.59 (50.45)	3.00 (2.95)	13.88 (13.74)	8.78 (8.62)	1.83	17	13.23-26.99
1b	$[Co(L)_2]$	802.57	>300 (61)	7.34 (7.21)	50.88 (50.79)	3.01 (2.97)	13.96 (13.86)	8.83 (8.71)	4.77	19	15.18-32-52
1c	$[Ni(L)_2]$	802.33	282 (64)	7.32 (7.20)	50.90 (50.81)	3.02 (2.96)	13.97 (13.82)	8.84 (8.72)	2.98	19	28.79-41.98
1d	[Zn(L).Cl]	472.65	278 (71)	13.83 (13.67)	43.20 (43.04)	2.56 (2.51)	11.85 (11.73)	15.00 (14.81)	Diamag.	18	14.20-26.56
1e	[Cd(L).Cl]	519.68	>300 (75)	21.63 (21.51)	39.29 (39.12)	2.33 (2.29)	10.78 (10.69)	13.64 (13.57)	Diamag.	17	13.57-39.84

Table 2: Mass spectral data of ligand (HL) (1), (1a), (1b), (1d) & (1e)

Compound	Calculated m/z	Found m/z	Peak Assignment
HL (1)	395.0345	395.0348	$[M+Na]^+$
1a	807.19	806.00	$[M^{-1}]$
1b	802.57	802.00	[M]
1d	472.65	472.00	[M]
1e	519.68	520.00	[M]

Table 3: Thermal Decomposition of Ni(II) (1c) complex

Complex	Stage	Peak Temp. TG (^{0}C)	Loss of Mass (%)		Probable Assignments
			Practical	Theoretical	
1c	--	--	--	--	$Ni(C_{34}H_{24}N_8O_4S_2Cl_2)$
					$\downarrow$ —NH_3
	I	140	2.0	2.12	$Ni(C_{34}H_{21}N_7O_4S_2Cl_2)$
					$\downarrow$ —2CO —HCl
	II	336	11.83	11.73	$Ni(C_{32}H_{20}N_7O_4S_2Cl)$
					$\downarrow$ —$C_{22}H_{14}N_5OS$
	III	440	58.66	59.39	$Ni(C_{10}H_6N_2O_3SCl)$
					$\downarrow$
					NiO

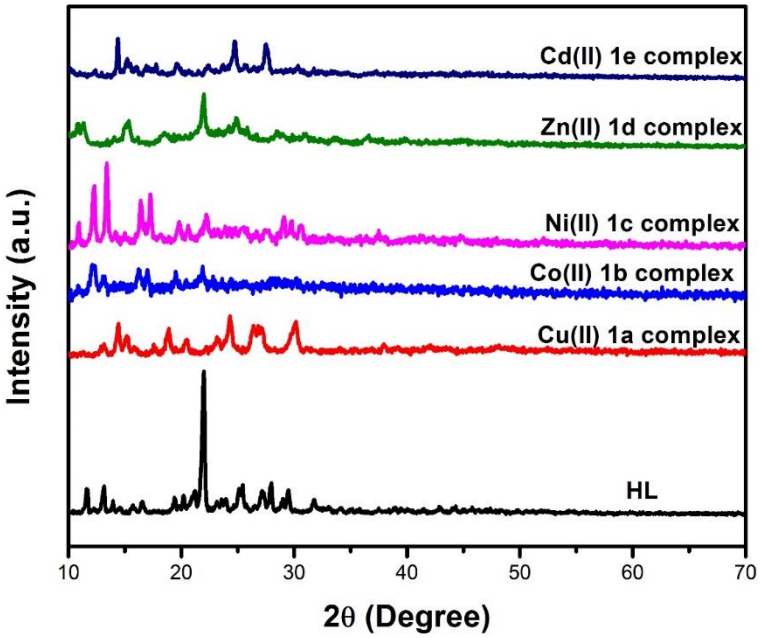

Figure 2: X-Ray diffraction pattern of Ligand (HL) (1) and its Cu(II), Co(II), Ni(II), Zn(II) and Cd(II) complexes

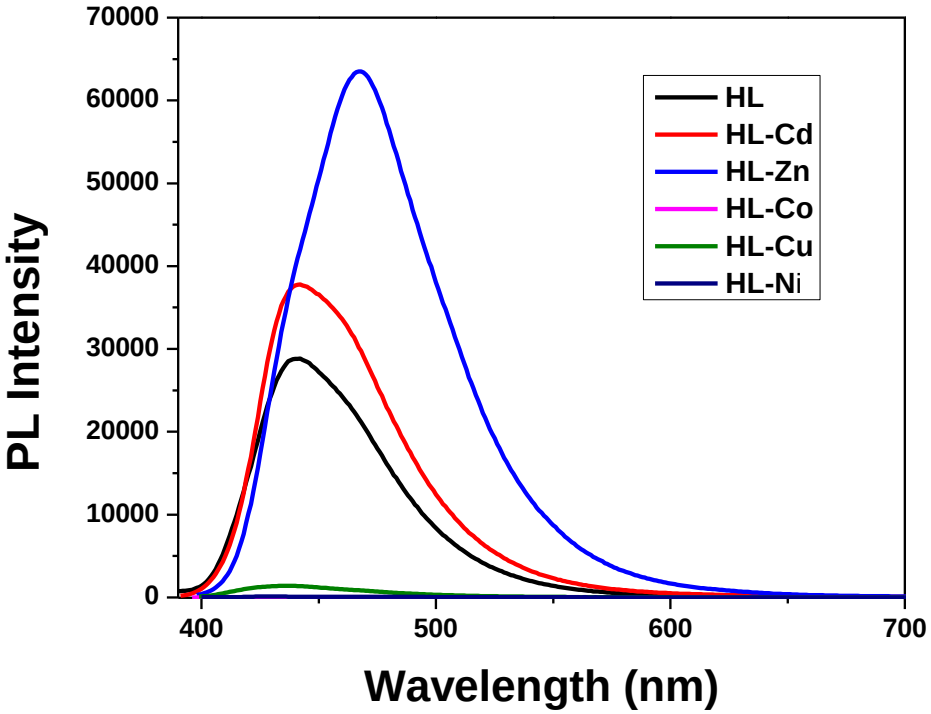

Fig 3: Fluorescence spectra of the ligand (HL) (1) and its complexes.

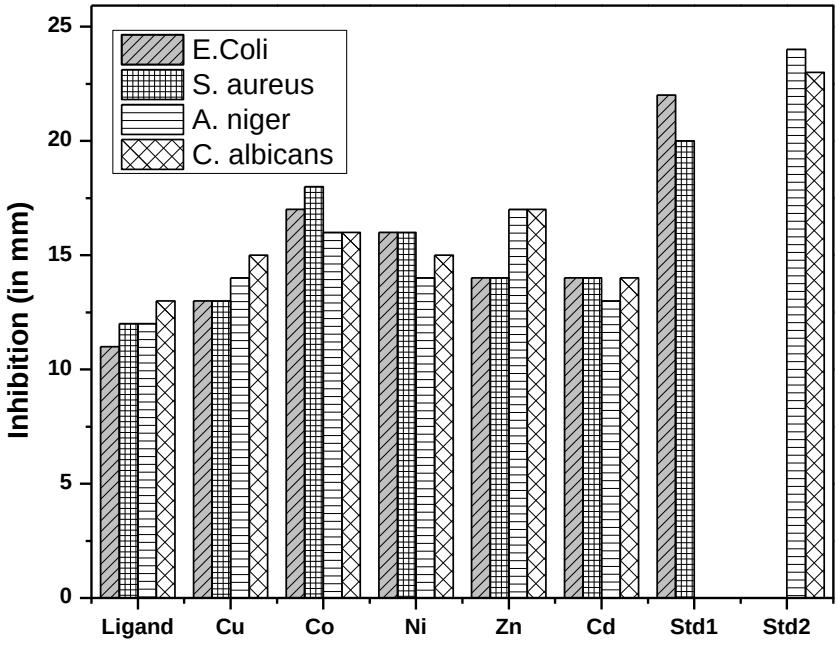

Fig 4: Antimicrobial screening data of the ligand (HL) (1) and its complexes.

SUPPORTING INFORMATION

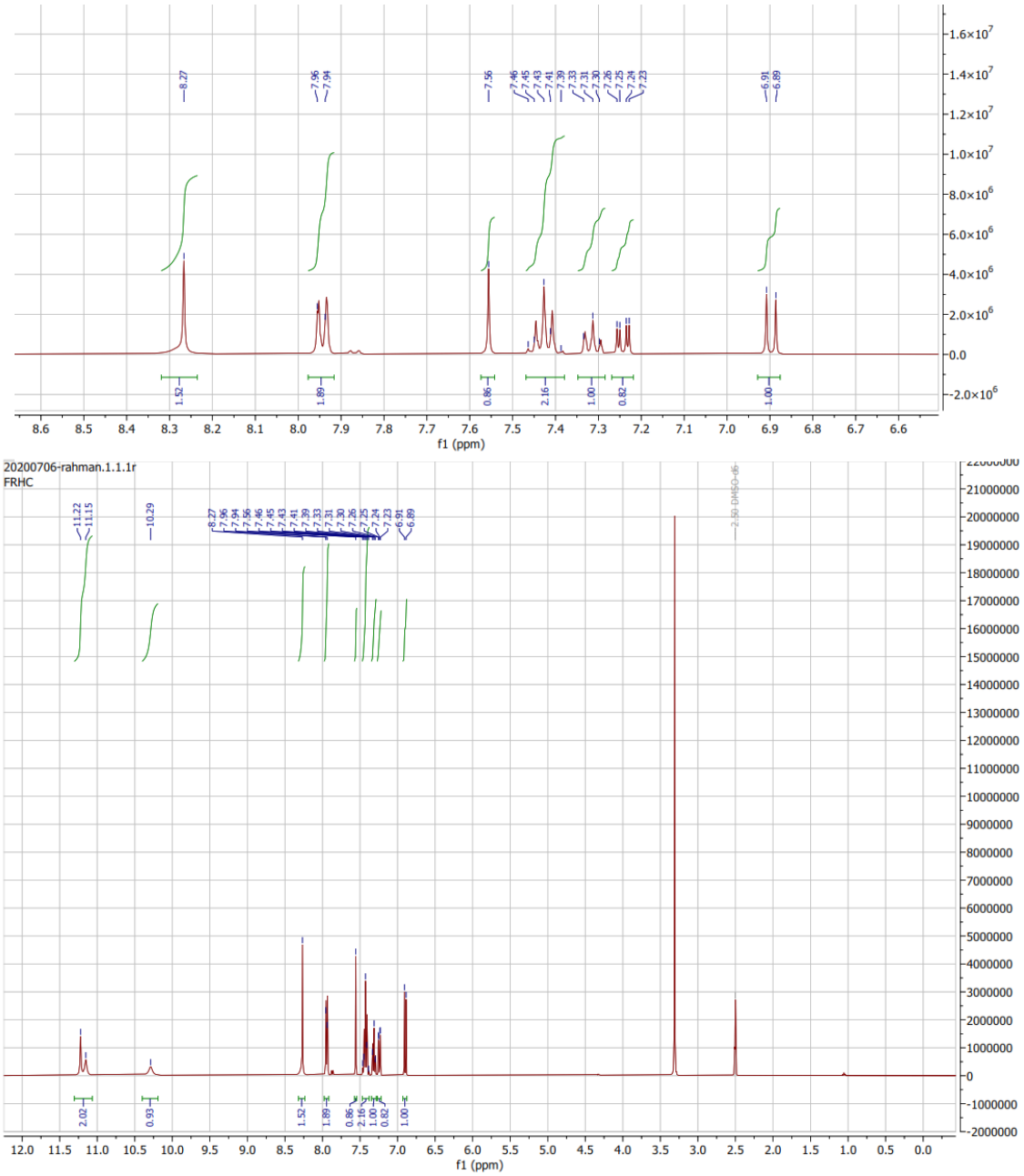

Figure S1: ^{1}H NMR spectrum of ligand (HL) (1)

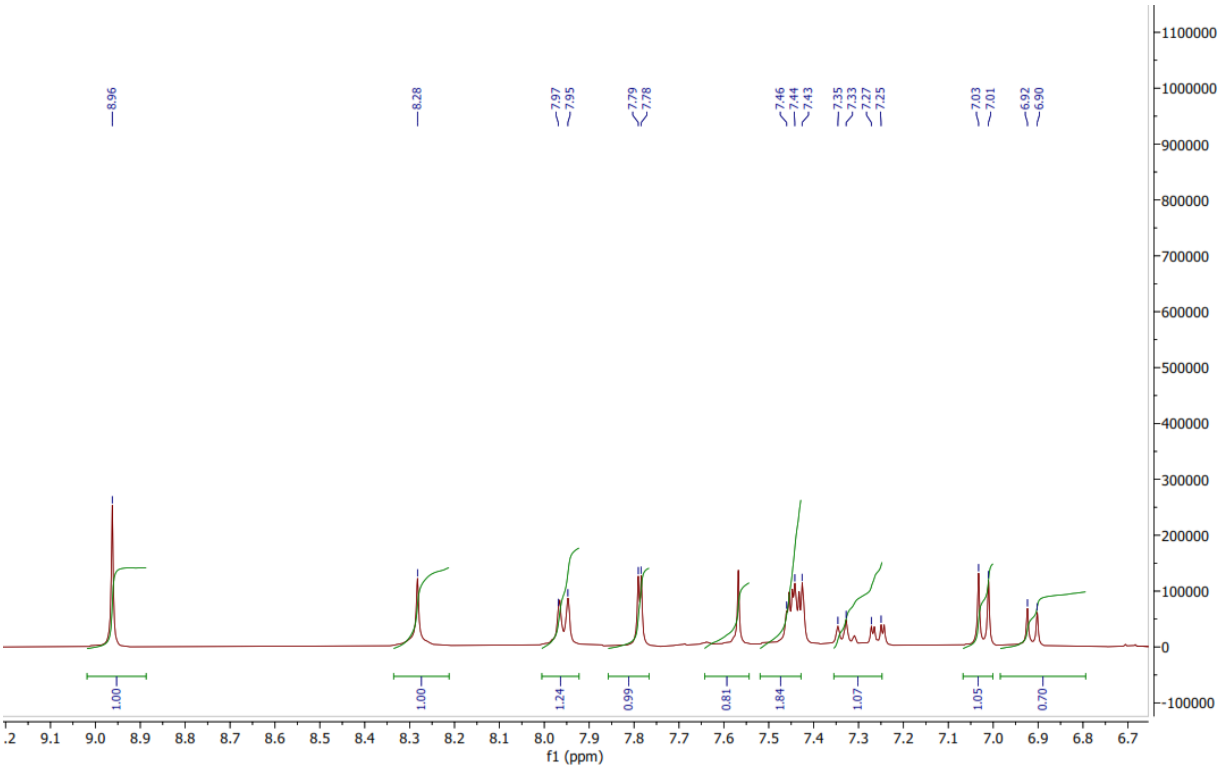

Figure S2: ^{1}H NMR spectrum of Cd (II) complex (1e)

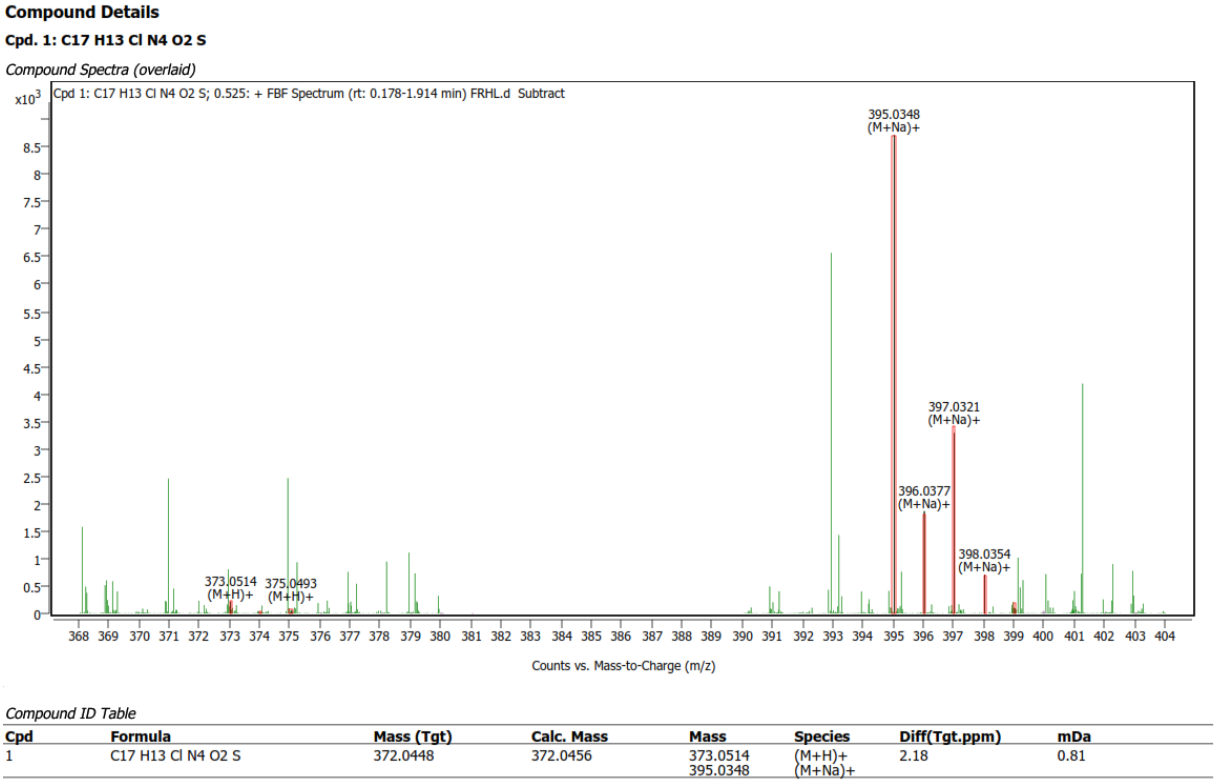

Figure S3: ESI mass spectrum of ligand (HL) (1)

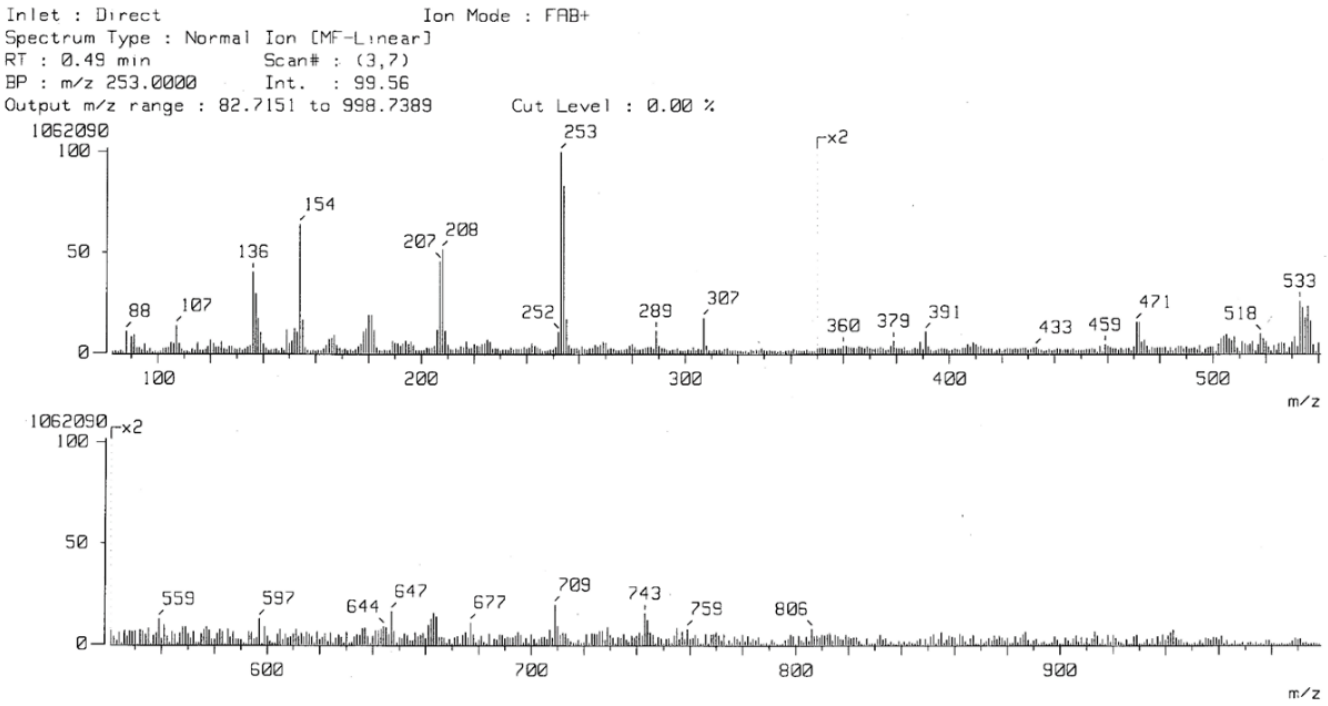

Figure S4: FAB mass spectrum of Cu(II) complex (1a)

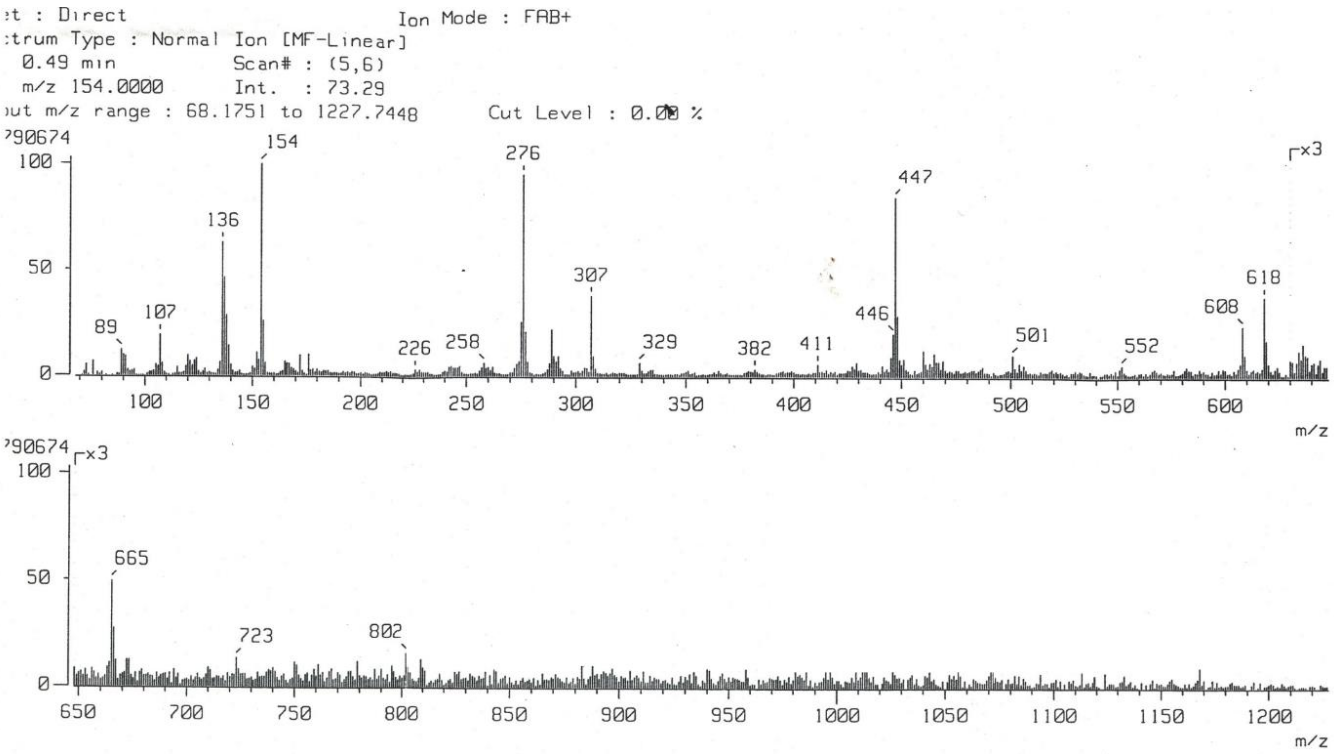

Figure S5: FAB mass spectrum of Co(II) complex (1b)

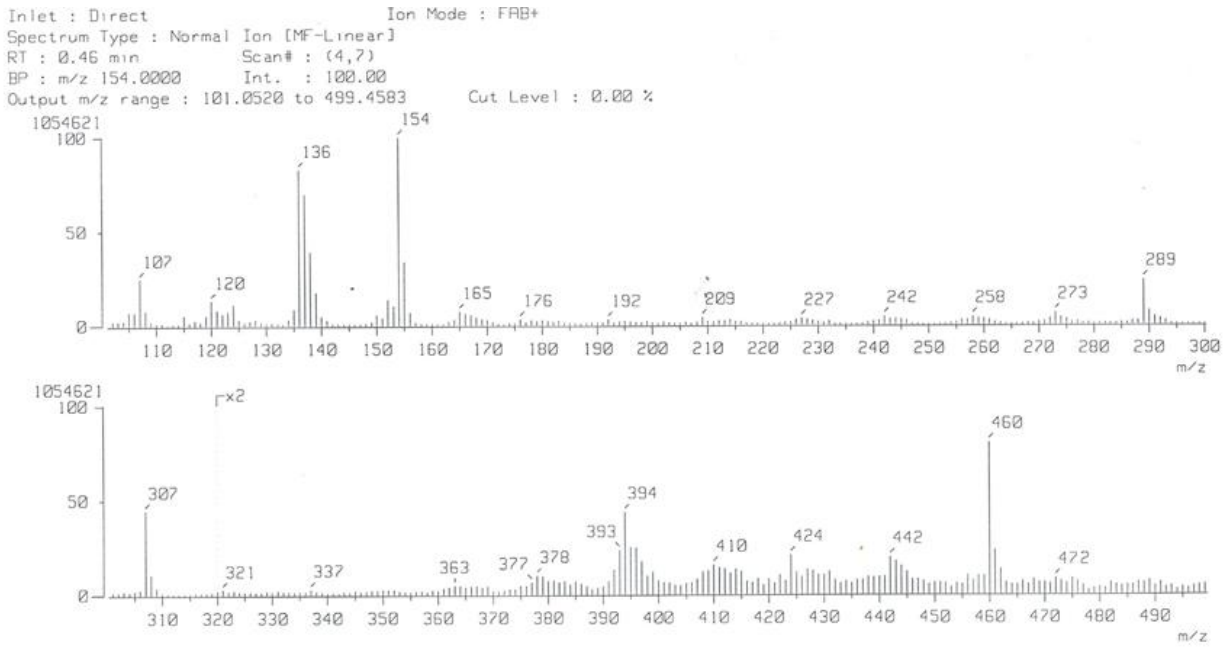

Figure S6: FAB mass spectrum of Zn(II) complex (1d)

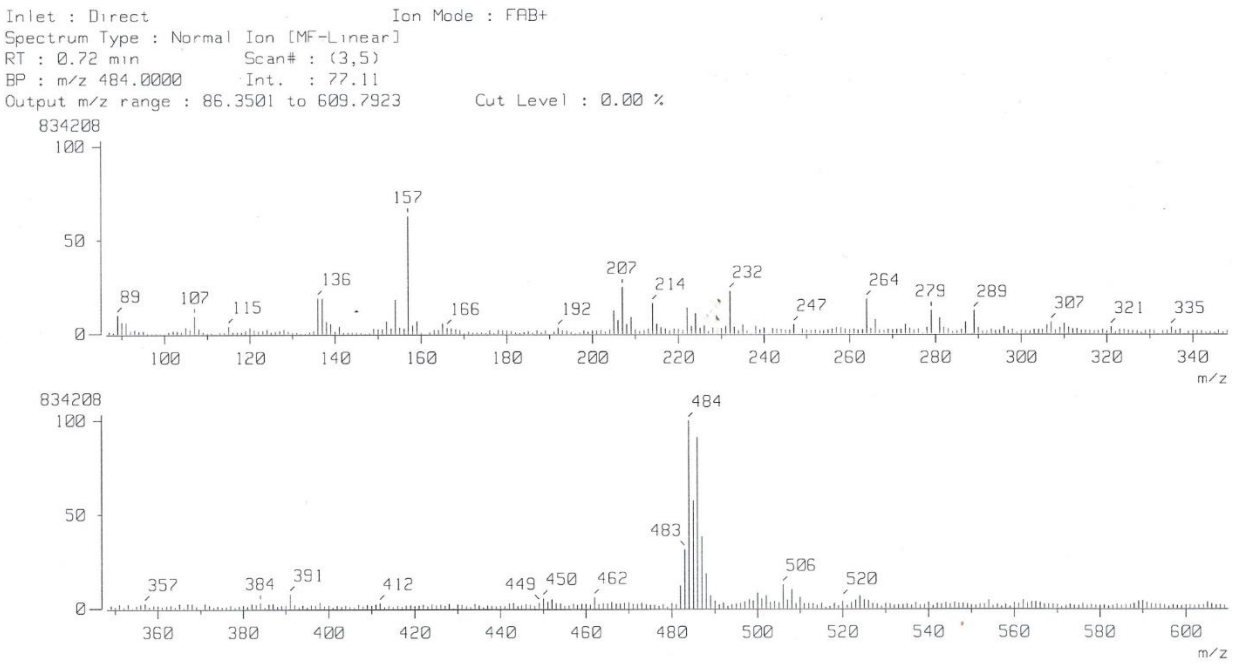

Figure S7: FAB mass spectrum of Cd(II) complex (1e)

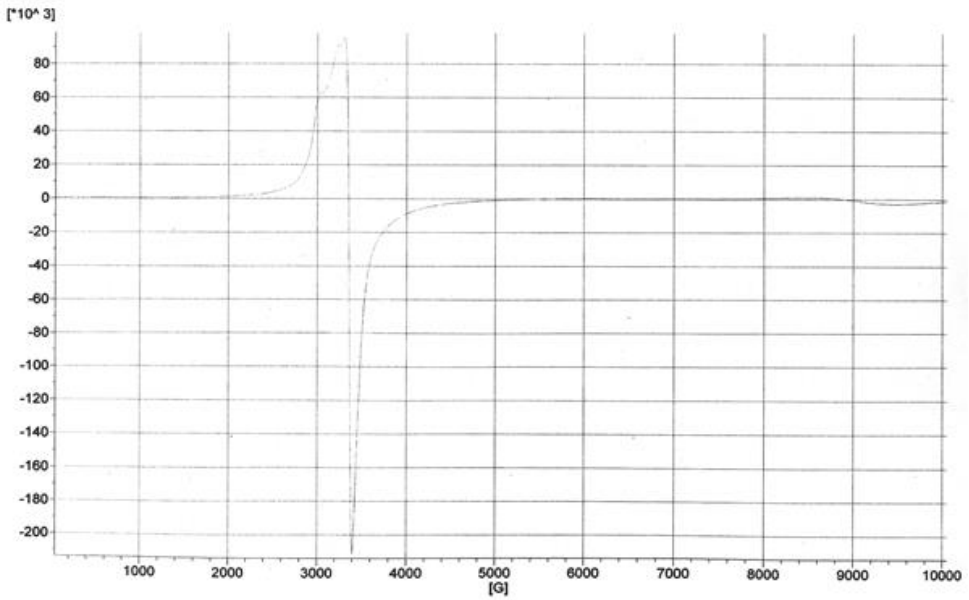

Figure S8: ESR spectrum of Cu(II) complex (1a)

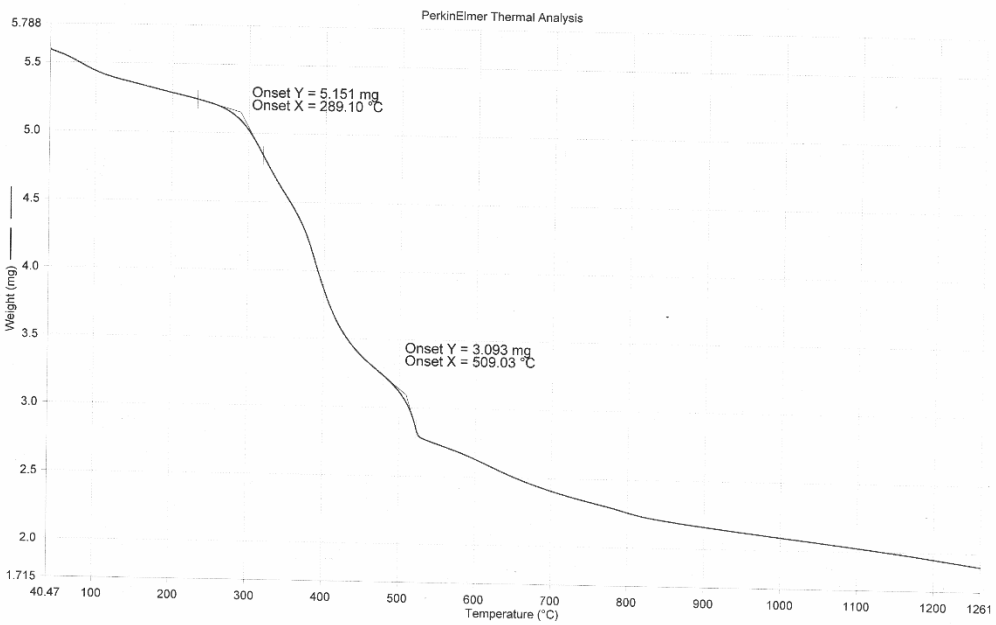

Figure S9: TGA of Ni(II) complex (1c)

Table: S1- Powder X-ray diffraction data of the Ligand HL

Sl No	2θ	θ	sinθ	$sin^2θ$	$h^2+k^2+l^2$	hkl	d		a (Å)
							Observed	Calculated	
1	7.24	3.62	0.06311	0.00398	3	111	12.2000	12.20627	21.13364
2	12.672	6.336	0.1103	0.01217	9	300	6.98000	6.98348	20.9423
3	14.485	7.2425	0.12601	0.01588	12	222	6.11000	6.11322	21.16858
4	15.784	7.892	0.13724	0.01883	14	321	5.61000	5.61291	20.99342
5	16.842	8.421	0.14637	0.02142	16	400	5.26000	5.26262	21.04229
6	18.988	9.494	0.16486	0.02718	20	420	4.67000	4.67241	20.8875
7	20.027	10.0135	0.17379	0.0302	23	--	4.43000	4.43229	21.24822
8	21.086	10.543	0.18288	0.03345	25	500	4.21000	4.21201	21.05186
9	21.82	10.91	0.18917	0.03579	27	511	4.07000	4.07195	21.15026
10	22.263	11.1315	0.19296	0.03724	28	--	3.99000	3.99192	21.11503
11	23.022	11.511	0.19946	0.03978	30	521	3.86000	3.862	21.1448
12	24.165	12.0825	0.20922	0.04377	33	522	3.68000	3.68185	21.14239
13	25.502	12.751	0.2206	0.04867	37	610	3.49000	3.49177	21.23134
14	27.335	13.6675	0.23617	0.05578	42	541	3.26000	3.26164	21.12961
15	29.16	14.58	0.25161	0.06331	48	444	3.06000	3.06152	21.2026
16	29.555	14.7775	0.25494	0.06499	49	700	3.02000	3.0215	21.14226
17	32.09	16.045	0.27626	0.07632	58	730	2.78700	2.78836	21.22723
18	32.692	16.346	0.2813	0.07913	60	--	2.73700	2.73837	21.20309
19	33.863	16.9315	0.29108	0.08473	64	800	2.64500	2.64631	21.16221
20	40.74	20.37	0.34791	0.12104	91	931	2.21300	2.21406	21.1126

Table: S2- Powder X-ray diffraction data of the Cu(II) (1a) complex

Sl No	2θ	θ	sinθ	$\sin^2\theta$	$h^2+k^2+l^2$	hkl	d		a (Å)
							Observed	Calculated	
1	15.238	7.619	0.13252	0.01756	3	111	5.81000	5.81278	10.06412
2	15.672	7.836	0.13627	0.01857	3	111	5.65000	5.65277	9.78708
3	19.154	9.577	0.16629	0.02765	5	210	4.63000	4.63229	10.35407
4	23.205	11.6025	0.20102	0.04041	7	--	3.83000	3.83196	10.13445
5	24.232	12.116	0.20979	0.04401	8	220	3.67000	3.67182	10.38144
6	24.641	12.3205	0.21327	0.04549	8	220	3.61000	3.6118	10.21172
7	31.138	15.569	0.26827	0.07197	12	222	2.87000	2.8714	9.94296
8	41.989	20.9945	0.3581	0.12824	22	332	2.15000	2.15105	10.08537
9	48.652	24.326	0.41173	0.16952	29	520	1.87000	1.87088	10.07106

Table: S3- Powder X-ray diffraction data of the Co(II) (1b) complex

Sl No	2θ	θ	sinθ	$\sin^2\theta$	$h^2+k^2+l^2$	hkl	d		a (Å)
							Observed	Calculated	
1	4.106	2.053	0.03581	0.00128	3	111	21.50000	21.51328	37.24758
2	8.257	4.1285	0.07196	0.00518	12	222	10.70000	10.70498	37.0687
3	12.457	6.2285	0.10844	0.01176	28	-	7.10000	7.10353	37.5737
4	13.204	6.602	0.11491	0.01321	31	-	6.70000	6.70329	37.30778
5	14.274	7.137	0.12418	0.01542	36	442	6.20000	6.20311	37.20418
6	14.752	7.376	0.12832	0.01646	39	-	6.00000	6.00317	37.4752
7	16.402	8.201	0.14257	0.02033	48	444	5.40000	5.40279	37.41707
8	17.038	8.519	0.14806	0.02192	51	711	5.20000	5.20252	37.13896
9	19.28	9.64	0.16737	0.02801	66	811	4.60000	4.6023	37.37467
10	19.713	9.8565	0.1711	0.02927	69	821	4.50000	4.50217	37.38328
11	20.693	10.3465	0.17951	0.03222	76	662	4.30000	4.29111	37.39447

Table: S4- Powder X-ray diffraction data of the Ni(II) (1c) complex

Sl. No	2θ	θ	sinθ	$\sin^2\theta$	$h^2+k^2+l^2$	hkl	d		a (Å)
							Observed	Calculated	
1	13.461	6.7305	0.11714	0.01372	3	111	6.57260	6.57588	11.38532
2	16.721	8.3605	0.14533	0.02112	5	210	5.29770	5.30043	11.84751
3	20.861	10.4305	0.18095	0.03274	7	-	4.25470	4.25693	11.2584
4	23.062	11.531	0.1998	0.03992	9	300	3.85350	3.85539	11.56167
5	25.322	12.661	0.21907	0.04799	10	310	3.51440	3.51618	11.11481

Table: S5- Powder X-ray diffraction data of the Zn(II) (1d) complex

Sl. No	2θ	θ	sinθ	$\sin^2\theta$	$h^2+k^2+l^2$	hkl	d		a (Å)
							Observed	Calculated	
1	7.818	3.909	0.06814	0.00464	3	111	11.30000	11.30508	19.57335
2	10.996	5.498	0.09576	0.00917	6	211	8.04000	8.04385	19.69566
3	15.898	7.949	0.13822	0.01911	12	222	5.57000	5.57292	19.29765
4	18.705	9.3525	0.16243	0.02638	17	322 410	4.74000	4.74246	19.54604
5	19.713	9.8565	0.1711	0.02927	19	331	4.50000	4.50217	19.61687
6	22.039	11.0195	0.19105	0.0365	24	422	4.03000	4.03198	19.74492
7	24.099	12.0495	0.20865	0.04354	28	-	3.69000	3.69179	19.52749
8	25.428	12.714	0.21997	0.04839	31	-	3.50000	3.50176	19.48941
9	28.587	14.2935	0.24677	0.06089	39	-	3.12000	3.12157	19.48663

Table: 9- Powder X-ray diffraction data of the Cd(II) (1e) complex

Sl. No	2θ	θ	sinθ	$\sin^2\theta$	$h^2+k^2+l^2$	hkl	d		a (Å)
							Observed	Calculated	
1	7.818	3.909	0.06814	0.00464	3	111	11.30000	11.30508	19.57335
2	15.398	7.699	0.1339	0.01793	12	222	5.75000	5.75274	19.92032
3	19.891	9.9455	0.17262	0.0298	19	331	4.46000	4.46228	19.44306
4	22.549	11.2745	0.19541	0.03819	25	430	3.94000	3.94193	19.70198
5	24.993	12.4965	0.21627	0.04677	30	521	3.56000	3.56172	19.50074